## TOP-DOWN BEATS BOTTOM-UP IN 3D INSTANCE SEGMENTATION

Maksim Kolodiazhnyi\*

Danila Rukhovich\*

Anna Vorontsova

Anton Konushin

Samsung AI Center Moscow, Russia

#### **ABSTRACT**

Most 3D instance segmentation methods exploit a bottom-up strategy, typically including resource-exhaustive post-processing. For point grouping, bottom-up methods rely on prior assumptions about the objects in the form of hyperparameters, which are domain-specific and need to be carefully tuned. On the contrary, we address 3D instance segmentation with a TD3D: top-down, fully data-driven, simple approach trained in an end-to-end manner. With its straightforward fully-convolutional pipeline, it performs surprisingly well on the standard benchmarks: ScanNet v2, its extension ScanNet200, and S3DIS. Besides, our method is much faster on inference than the current state-of-the-art grouping-based approaches. Code is available at https://github.com/SamsungLabs/td3d.

*Index Terms*— 3D instance segmentation, indoor scene understanding, point clouds

## 1. INTRODUCTION

With the emergence of AR/VR, 3D indoor scanning, and household robotics, 3D instance segmentation becomes a key technology facilitating scene understanding. It is a holistic and challenging task of finding objects in 3D point clouds, predicting their semantic labels, and assigning an instance ID for each object.

Two major 3D instance segmentation paradigms have been introduced so far [1]. *Bottom-up* methods learn perpoint embeddings and use them to cluster points so that they form a set of proposals. *Top-down* directly predict instance proposals as object proxies, which are then filtered via non-maximum suppression, and refined via mask segmentation individually.

In 2D instance segmentation, most state-of-the-art methods follow the top-down paradigm. Unfortunately, 2D methods that work well on a pixel grid cannot be directly adapted to process unstructured and sparse 3D points, and bottom-up methods dominate the field of 3D point cloud processing. Accordingly, the recent progress in 3D instance segmentation has been associated with improving components of bottom-up approaches: different ways of selecting points to be grouped

have been studied [2], advanced feature aggregation strategies have been proposed [3, 4], with estimates being refined via elaborate post-processing schemes [5, 6]. In the meantime, top-down methods have been out of the spotlight.

Nevertheless, bottom-up 3D instance segmentation methods have crucial drawbacks, limiting their performance. Besides being computationally-expensive, bottom-up approaches are sensitive to the values of numerous hyperparameters. Particularly, they might fail to find a proper balance between over-fragmented and accidentally merged masks and have limited generalization ability to complex scenes with objects of varying scales.

Our goal is to prove the top-down paradigm has great potential, which is yet unleashed in the 3D domain. In this paper, we tackle the challenging 3D instance segmentation task with TD3D, a top-down, fully-convolutional, simple approach trained end-to-end in a fully data-driven way. We conduct extensive experiments on the ScanNet v2, ScanNet200, and S3DIS datasets, and report competitive results for all these benchmarks.

## 2. RELATED WORK

**Bottom-up methods.** Up until very recently, grouping-based bottom-up methods have dominated the field. In SGPN [7], a similarity matrix for all 3D point pairs is learned, and the most similar points are assembled into instances. 3D-SIS [8] utilizes RGB images as an additional source of data and merges 3D features from a point cloud with backprojected 2D features extracted from RGB images. ASIS [9] uses spatial discriminative loss to learn point-level embeddings and generates instance masks via a mean-shift algorithm. 3D-MPA [10] predicts instance centers and refines initial instance proposals with a graph convolutional network. Additional estimates are used to guide clustering, e.g., OccuSeg [11] predicts occupancy, while PointGroup [5] assigns 3D points with semantic labels and center votes. In HAIS [3], clustering is performed in a hierarchic manner. SSTNet [4] aggregates point-wise semantic and instance-level features, using a semantic superpoint tree (SST) with superpoints as leaves. SoftGroup [6] leverages a 3D sparse network to group 3D points according to the predicted soft semantic scores and refines the obtained proposals with a 3D U-Net-like network. DyCo3D [2] also

<sup>\*</sup>Equal contribution

employs refinement, yet incorporates dynamic convolutions. **Top-down methods.** Top-down 3D instance segmentation

methods directly generate object proposals and then predict or

refine masks for each proposal. 3D-BoNet [12] applies Hun-

garian matching and outputs a fixed set of proposals in the form of non-oriented 3D bounding boxes. Instead of regressing 3D bounding boxes, GSPN [13] employs an analysis-bysynthesis strategy to predict instance shapes. NeuralRF [1] generates the affinity of points in the point cloud to a query point and uses coordinate networks representing convex domains to model the spatial affinity in the neural bilateral filter. **3D** object detection. Modern 3D object detection methods can be categorized into voting-based, transformer-based, and 3D convolutional. Voting-based methods extract per-point features, merge them into an object proposal, and accumulate features of points within each group; overall, they use point grouping similar to bottom-up 3D instance segmentation methods. Instead of domain-specific heuristics and hyperparameters, transformer-based methods use end-to-end learning and forward pass on inference. Both voting- and transformer-based methods have scalability issues, making them impractical. Differently, top-down 3D convolutional methods represent point clouds as voxels, which makes them more memory-efficient and allows scaling to large scenes without sacrificing point density. Up until very recently, such methods lacked accuracy, yet the last advances in the field allowed developing fast, scalable, and accurate methods [14].

## 3. PROPOSED METHOD

The proposed method runs in two stages. First, it detects objects in a point cloud and extracts corresponding bounding boxes. These bounding boxes are interpreted as initial object proposals and then refined with a lightweight network to obtain final instance masks (Fig. 1). All operations within the pipeline are implemented through 3D sparse convolutions.

# 3.1. Proposal Generation

We obtain object proposals with a 3D object detection method that outputs 3D object bounding boxes alongside object categories and confidence scores. Any conventional 3D object detection method can be employed for this purpose. We aim to avoid point grouping and follow a top-down paradigm at each stage of our pipeline, so we narrowed our search to the 3D convolutional-based methods. As the result, we opted for fast and efficient, fully-convolutional FCAF3D [14].

Given a predicted bounding box, the RoI extractor selects voxels whose centers are inside this bounding box. These voxels with corresponding features from the backbone serve as initial object proposals.

### 3.2. Proposal Refinement

Our proposal refinement module takes voxels with features from RoI extractor as inputs and predicts final instance masks. For this purpose, we consider a 3D tiny U-Net network (a U-Net style network with few layers) solving a binary segmentation task, that classifies voxels into *foreground* and *background*. For each voxel, all points inside this voxel are assigned with the same *foreground* or *background* label predicted by U-Net, which gives final per-point instance masks.

## 3.3. Training Procedure

We train our method end-to-end, updating both proposal generation and proposal refinement models simultaneously. The total loss is a sum of two proposal generation losses  $\mathcal{L}_{cls}$ ,  $\mathcal{L}_{reg}$  and a proposal refinement loss  $\mathcal{L}_{seg}$ :

$$\mathcal{L} = \mathcal{L}_{cls} + \mathcal{L}_{reg} + \mathcal{L}_{seg}$$

Proposal generation. Our proposal generation model is inherited from FCAF3D [14], accordingly, we follow the original training procedure and use focal loss  $\mathcal{L}_{cls}$  and IoU loss  $\mathcal{L}_{reg}$  to penalize classification and regression errors, respectively. During training, this model outputs 3D object bounding boxes parameterized with their centers and sizes (length, width, height), which we consider as initial object proposals. **Proposal refinement.** For training the proposal refinement model, a correspondence between proposals and ground truth instances should be established. Specifically, we calculate centers of 3D bounding boxes of ground truth instances and match ground truth instances with the nearest proposal according to center-center distance, similar to FCAF3D [14]. Then, we filter such correspondences by IoU, keeping only the proposals for which IoU with ground truth exceeds the pre-defined threshold. Our binary segmentation model is trained via minimizing  $\mathcal{L}_{seg}$ , which is calculated as a BCE loss between predicted and ground truth instance masks.

#### 4. EXPERIMENTS

## 4.1. Experimental Settings

**Datasets.** The experiments are conducted on ScanNet v2 [18], ScanNet200 [17], and S3DIS [19]. ScanNet v2 [18] contains 1613 scans divided into training, validation, and testing splits of 1201, 312, and 100 scans, respectively. 3D instance segmentation is typically evaluated using 18 object classes. We report results on both validation and hidden test splits. ScanNet200 [17] extends the original ScanNet semantic annotation with fine-grained categories with the long-tail distribution. The training, validation, and testing splits are similar to the original ScanNet v2 dataset. The S3DIS dataset [19] features 271 scenes within 6 large areas.

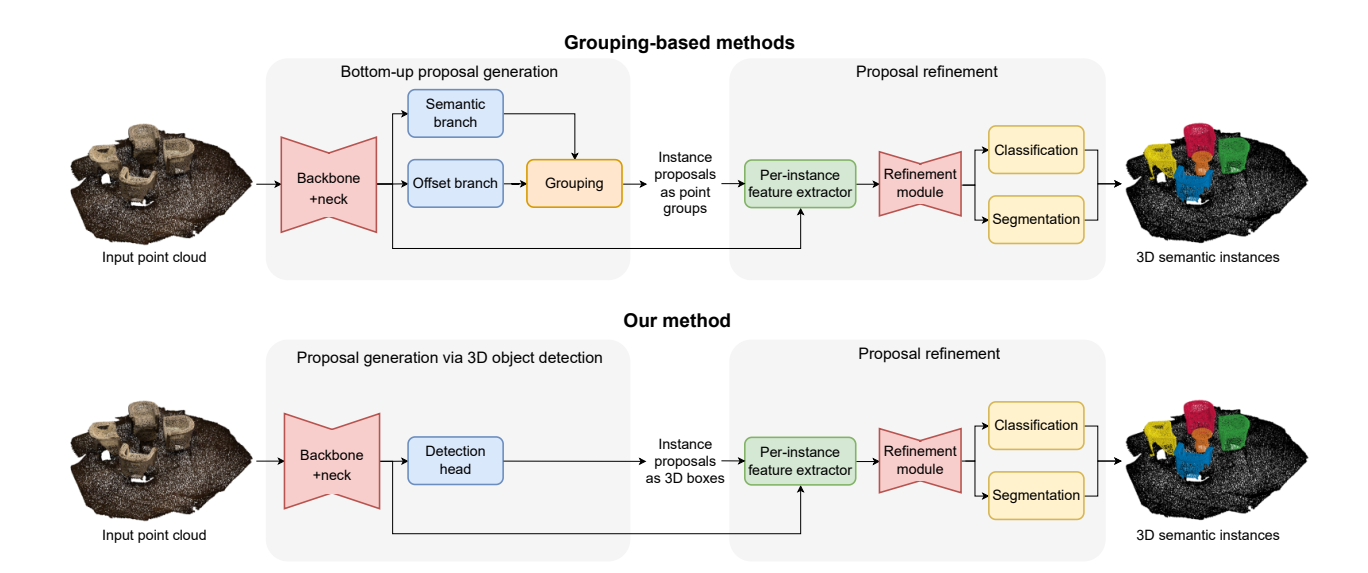


**Fig. 1**: Scheme of TD3D in comparison with state-of-the-art grouping-based methods (e.g., PointGroup [5], SoftGroup [6]). Our proposal refinement is the same as in SoftGroup [6], while proposal generation significantly differs. Specifically, bottom-up proposal generation returns *point groups*, while we leverage 3D object detection that outputs instance proposals as *3D object bounding boxes* instead.

Paradigm	Method	Conference	Validation			Test			Runtime
	1,10,110,0		AP	AP <sub>50</sub>	AP <sub>25</sub>	AP	AP <sub>50</sub>	AP <sub>25</sub>	(in sec)
Bottom-up	PointGroup [5]	CVPR'20	34.8	56.7	71.3	40.7	63.6	77.8	0.372
	SSTNet [4]	ICCV'21	49.4	64.3	74.0	50.6	69.8	78.9	0.419
	HAIS [3]	ICCV'21	43.5	64.4	75.6	45.7	69.9	80.3	0.256
	DyCo3D [2]	CVPR'21	35.4	57.6	72.9	39.5	64.1	76.1	0.267
	SoftGroup [6]	CVPR'22	45.8	<u>67.6</u>	<u>78.9</u>	<u>50.4</u>	76.1	<u>86.5</u>	0.266
Top-down	3D-SIS [8]	CVPR'19	-	18.7	35.7	16.1	38.2	55.8	>10
	GSPN [13]	CVPR'19	19.3	37.8	53.4	-	30.6	-	>10
	3D-BoNet [12]	NeurIPS'19	-	-	-	25.3	48.8	68.7	9.174
	NeuralRF [1]	WACV'23	36.0	55.5	71.1	35.3	55.5	71.8	-
	TD3D (ours)		<u>46.2</u>	71.1	81.3	48.9	<u>75.1</u>	87.5	0.151

Method	AP						
11201100	head	common	tail				
CSC [15]	22.3	8.2	4.6				
Mink34D [16]	24.6	8.3	4.3				
LGround [17]	27.5	10.8	6.0				
TD3D (ours)	33.2	<b>17.7</b>	10.3				

**Table 2**: Results for the ScanNet200 test split. AP scores for the most frequent (*head* of distribution), common, and rare (*tail*) object categories are provided. The best results are **bold**.

**Table 1**: Results for ScanNet v2. The best results are **bold**, the second best are <u>underlined</u>. The runtime is measured using a single NVidia 3090 GPU.

Following the standard evaluation protocol, we assess the segmentation quality on scans from Area 5, and via 6 cross-fold validation, using 5 semantic categories in both settings.

**Metrics.** We use the average precision as a major metric.  $AP_{50}$  and  $AP_{25}$  are the scores obtained with IoU thresholds of 50% and 25%, respectively, while AP is an average score with IoU threshold varying from 50% to 95% with a step of 5%.

**Implementation details.** Our models are implemented using Pytorch. We train for 330 epochs on a single NVidia 3090 GPU, using Adam optimizer. The batch size is 6, and the initial learning rate is set to 0.001 and is reduced by 10 times after 280 and 320 epochs. Other implementation details are similar to FCAF3D [14].

#### 4.2. Comparison to Prior Work

**ScanNet v2.** Results for validation and test splits of ScanNet v2 are presented in Tab. 1. Overall, TD3D is on par with previous state-of-the-art SoftGroup [6] on the test split and shows superior results on validation. Another advantage of TD3D is its inference speed: according to the reported runtime, it is more than 1.5x faster than any method that performs grouping.

**ScanNet200.** We evaluate TD3D on the test split of ScanNet200 and report metrics in Tab. 2. For either frequent, common, or rare categories, our method demonstrates a solid superiority over the existing approaches. The gain is especially tangible for less frequent categories, where TD3D improves

previous state-of-the-art metrics by approximately 1.7x times (+6.8 and +4.3 AP for common and tail, respectively).

**S3DIS.** According to the Tab. 3, TD3D surpasses other methods by at least +4.7 AP and +3.6 AP for Area 5 and 6-fold, respectively. Meanwhile, if being pre-trained on ScanNet and fine-tuned on S3DIS, as proposed in [3, 6], it outperforms the previous state-of-the-art SoftGroup [6] in terms of all metrics by a large margin.

Method	Area 5				6-fold CV				
Welloa	AP	AP <sub>50</sub>	Prec <sub>50</sub>	Rec <sub>50</sub>	AP	AP <sub>50</sub>	Prec <sub>50</sub>	Rec <sub>50</sub>	
SGPN [7]	-	-	36.0	28.7	-	-	38.2	31.2	
ASIS [9]	-	-	55.3	42.4	-	-	63.6	47.5	
3D-BoNet [12]	-	-	57.5	40.2	-	-	65.6	47.6	
OccuSeg [11]	-	-	-	-	-	-	72.8	60.3	
3D-MPA [10]	-	-	63.1	58.0	-	-	66.7	64.1	
PointGroup [5]	-	57.8	61.9	62.1	-	64.0	69.6	69.2	
DyCo3D [2]	-	-	64.3	64.2	-	-	-	-	
MaskGroup [20]	-	65.0	62.9	64.7	-	69.9	66.6	69.2	
SSTNet [4]	42.7	59.3	65.5	64.2	54.1	67.8	73.5	73.4	
TD3D (ours)	47.4	66.5	70.4	71.6	57.7	77.7	84.3	75.6	
HAIS [3]	-	-	71.1	65.0	-	-	73.2	69.4	
SoftGroup [6]	51.6	66.1	73.6	66.6	54.4	68.9	75.3	69.8	
TD3D (ours)	61.1	75.5	79.9	75.2	63.6	78.2	86.8	76.6	

**Table 3**: Results for S3DIS. The best results are **bold**. The scores, obtained via pre-training on ScanNet and fine-tuning on S3DIS, are depicted in light gray.

#### 4.3. Qualitative Results

The original and segmented point clouds from ScanNet and S3DIS datasets are depicted in Fig. 2.

## 4.4. Ablation Studies

In this section, we analyze different components of our approach and measure the contribution to the final quality of each component. The ablation experiments are conducted on the ScanNet v2 validation set, following the same evaluation protocol as for the qualitative comparison.

Number of feature levels in a tiny U-Net. We study how the size of the proposal refinement network affects the segmentation accuracy. Starting from 0 levels (all points in an initial proposal are included in the instance mask), and using no more than 4 levels (as in the backbone), we select the best option in terms of AP. As can be seen from Tab. 4, AP grows with the number of levels; yet, we do not want our refinement model to be large, so we opt for 4 levels in the final version.

**Number of initial proposals.** Furthermore, we investigate the dependency between the number of initial proposals, accuracy, and runtime. Note that the number of proposals are

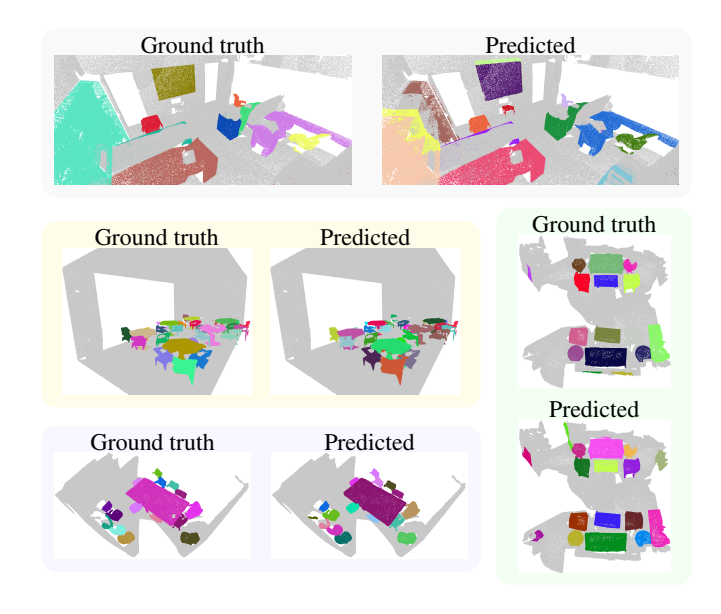


Fig. 2: 3D instance segmentation on ScanNet v2 and S3DIS.

approximate, since they cannot be set explicitly but manipulated through the NMS hyperparameters. As expected, the more proposals, the higher is AP (Tab. 5). However, with as many as 60 proposals, our method reaches the plateau in terms of segmentation accuracy. In the meantime, the inference time tends to increase with the growing number of proposals. Overall, we assume that with  $\approx 60$  initial proposals, our method demonstrates a decent trade-off between accuracy and speed, so we use this value by default in our experiments.

U-Net size	AP	• • • • • • • • • • • • • • • • • • • •	Initial	AP	Runtime	
0	25.8	pr	proposals		(in sec)	
1	37.9	;	≈140	46.6	0.260	
2	44.4	;	≈100	46.4	0.210	
3	45.5		$\approx$ 60	46.2	0.151	
4	46.2		$\approx 20$	44.6	0.105	

**Table 4**: Results of a study of the apof the tiny U-Net size on the ScanNet v2 validation set. **Table 5**: Results of a study of the apof the tiny U-Net size on the proximate number of initial proposals on the ScanNet v2 validation set.

#### 5. CONCLUSION

In this work, we introduced TD3D, a novel 3D instance segmentation method following a top-down paradigm. Being fully-convolutional and trained end-to-end in a data-driven way, it does not rely on prior assumptions about the objects, which eases the burden of manually tuning domain-specific hyperparameters. We evaluated our method on the standard benchmarks: ScanNet v2, its extension ScanNet200, and S3DIS. Our experiments demonstrated that TD3D is on par with state-of-the-art grouping-based 3D instance segmentation methods: being as accurate, it is more than 1.5x faster on inference.

#### 6. REFERENCES

- [1] Weiwei Sun, Daniel Rebain, Renjie Liao, Vladimir Tankovich, Soroosh Yazdani, Kwang Moo Yi, and Andrea Tagliasacchi, "Neuralbf: Neural bilateral filtering for top-down instance segmentation on point clouds," in Winter Conference on Computer Vision (WACV), 2023.
- [2] Tong He, Chunhua Shen, and Anton van den Hengel, "DyCo3d: Robust instance segmentation of 3d point clouds through dynamic convolution," in *IEEE Con*ference on Computer Vision and Pattern Recognition, 2021.
- [3] Shaoyu Chen, Jiemin Fang, Qian Zhang, Wenyu Liu, and Xinggang Wang, "Hierarchical aggregation for 3d instance segmentation," in *IEEE/CVF International Conference on Computer Vision*, 2021.
- [4] Zhihao Liang, Zhihao Li, Songcen Xu, Mingkui Tan, and Kui Jia, "Instance segmentation in 3d scenes using semantic superpoint tree networks," in *IEEE/CVF International Conference on Computer Vision*, 2021, pp. 2783–2792.
- [5] Li Jiang, Hengshuang Zhao, Shaoshuai Shi, Shu Liu, Chi-Wing Fu, and Jiaya Jia, "Pointgroup: Dual-set point grouping for 3d instance segmentation," in *IEEE Con*ference on Computer Vision and Pattern Recognition, 2020.
- [6] Thang Vu, Kookhoi Kim, Tung M. Luu, Xuan Thanh Nguyen, and Chang D. Yoo, "Softgroup for 3d instance segmentation on 3d point clouds," in *IEEE Conference on Computer Vision and Pattern Recognition*, 2022.
- [7] Weiyue Wang, Ronald Yu, Qiangui Huang, and Ulrich Neumann, "Sgpn: Similarity group proposal network for 3d point cloud instance segmentation," in *IEEE Conference on Computer Vision and Pattern Recognition*, 2018, pp. 2569–2578.
- [8] Ji Hou, Angela Dai, and Matthias Nießner, "3d-sis: 3d semantic instance segmentation of rgb-d scans," in *IEEE Conference on Computer Vision and Pattern Recognition*, 2019.
- [9] Xinlong Wang, Shu Liu, Xiaoyong Shen, Chunhua Shen, and Jiaya Jia, "Associatively segmenting instances and semantics in point clouds," in *IEEE Con*ference on Computer Vision and Pattern Recognition, 2019, pp. 4091–4100.
- [10] Francis Engelmann, Martin Bokeloh, Alireza Fathi, Bastian Leibe, and Matthias Nießner, "3D-MPA: Multi Proposal Aggregation for 3D Semantic Instance Segmentation," in *IEEE Conference on Computer Vision* and Pattern Recognition, 2020.

- [11] Lei Han, Tian Zheng, Lan Xu, and Lu Fang, "Occuseg: Occupancy-aware 3d instance segmentation," in *IEEE Conference on Computer Vision and Pattern Recognition*, 2020, pp. 2937–2946.
- [12] Bo Yang, Jianan Wang, Ronald Clark, Qingyong Hu, Sen Wang, Andrew Markham, and Niki Trigoni, "Learning object bounding boxes for 3d instance segmentation on point clouds," in *Advances in Neural In*formation Processing Systems, 2019, pp. 6737–6746.
- [13] Li Yi, Wang Zhao, He Wang, Minhyuk Sung, and Leonidas Guibas, "Gspn: Generative shape proposal network for 3d instance segmentation in point cloud," in *IEEE Conference on Computer Vision and Pattern Recognition*, 2019, pp. 3942–3951.
- [14] Danila Rukhovich, Anna Vorontsova, and Anton Konushin, "Fcaf3d: fully convolutional anchor-free 3d object detection," in *IEEE/CVF European Conference on Computer Vision*, 2022, pp. 477–493.
- [15] Ji Hou, Benjamin Graham, Matthias Nießner, and Saining Xie, "Exploring data-efficient 3d scene understanding with contrastive scene contexts," in *IEEE Conference on Computer Vision and Pattern Recognition*, 2021, pp. 15587–15597.
- [16] Christopher Choy, Jun Young Gwak, and Silvio Savarese, "4d spatio-temporal convnets: Minkowski convolutional neural networks," in *IEEE Conference on Computer Vision and Pattern Recognition*, 2019.
- [17] David Rozenberszki, Or Litany, and Angela Dai, "Language-grounded indoor 3d semantic segmentation in the wild," in *IEEE/CVF European Conference on Computer Vision*, 2022.
- [18] Angela Dai, Angel X. Chang, Manolis Savva, Maciej Halber, Thomas Funkhouser, and Matthias Nießner, "Scannet: Richly-annotated 3d reconstructions of indoor scenes," in *IEEE Conference on Computer Vision and Pattern Recognition*, 2017.
- [19] Iro Armeni, Ozan Sener, Amir R. Zamir, Helen Jiang, Ioannis Brilakis, Martin Fischer, and Silvio Savarese, "3d semantic parsing of large-scale indoor spaces," in *IEEE Conference on Computer Vision and Pattern Recognition*, 2016, pp. 1534–1543.
- [20] Shaoyu Chen, Jiemin Fang, Qian Zhang, Wenyu Liu, and Xinggang Wang, "Hierarchical aggregation for 3d instance segmentation," in *IEEE/CVF International Conference on Computer Vision*, 2021, pp. 15467–15476.